MULTIVARIATE OPTIMIZATION FOR MULTIFRACTAL-BASED TEXTURE SEGMENTATION

Jordan Frecon[1]*, Nelly Pustelnik*[1]*, Herwig Wendt*[2]*, Patrice Abry*[1]*,*

[1] Physics Dept. - ENSL, UMR CNRS 5672, F-69364 Lyon, France, firstname.lastname@ens-lyon.fr

[2] IRIT, CNRS UMR 5505, INP-ENSEEIHT, F-31062 Toulouse, France, firstname.lastname@irit.fr

ABSTRACT

This work aims to segment a texture into different regions, each characterized by a priori unknown multifractal properties. The multifractal properties are quantified using the multiscale function $C_{1,j}$ that quantifies the evolution along analysis scales 2^j of the empirical mean of the log of the wavelet leaders. The segmentation procedure is applied to local estimate of $C_{1,j}$. It involves a multivariate Mumford-Shah relaxation formulated as a convex optimization problem involving a structure tensor penalization and an efficient algorithmic solution based on primal-dual proximal algorithm. The performances are evaluated on synthetic textures.

***Index Terms*—** Local regularity, multifractal spectrum, segmentation, convex optimization, wavelet Leaders

1. INTRODUCTION

Multifractal texture characterization. Multidimensional multifractal analysis is now considered as a classical tool for texture characterization (cf. e.g. [1]). It notably permits to capture in a refined manner the detailed fluctuations of regularity of a texture along space and thus grounds texture characterization on the measurement of global and local smoothness. Local regularity is technically measured via the concept of Hölder exponent, and the multifractal spectrum provides practitioners with a global and geometrical characterization of the statistical fluctuations of Hölder exponents measured across the texture of interest. Multifractal tools have been used to characterize real-world textures from a large variety of applications of different natures ranging from biomedical (cf. e.g., [2]) to art investigations [3, 4]. It is also well documented that multifractal analysis should be grounded on wavelet leaders, consisting of local supremum of 2D wavelet transform coefficients taken across all finer scales [5, 1].

Texture segmentation. However, in its current formulation, multifractal analysis, as most texture characterization procedures, assumes a priori that the texture to analyze consists of a single piece with homogeneous properties, that is, texture properties of any subpart of the image available are identical. In most applications, however, texture analysis combines two different issues: Segmentation of the images into pieces or regions, of a priori unknown boundaries, where texture properties can be considered homogeneous and characterization of texture properties in each different homogeneous parts.

Solutions for image segmentation have been envisaged in many different ways [6, 7, 8, 9, 10, 11]. However, none of these algorithmic solutions appears to be robust to noise, unsupervised and exploiting the correlations through different components. To derive a new algorithmic solution satisfying all these constraints, we focus on a segmentation procedure derived from [12].

Goals and contributions. The present contribution elaborates on earlier works [13, 14, 15], aiming to segment a texture into local regularity piecewise constant regions, by proposing one of the first and rare attempt to segment a texture into regions, with unknown boundaries, and within which multifractal properties can be considered homogeneous. The proposed procedure thus aims to segment a texture into different regions, each characterized by a different a priori unknown multifractal spectrum. To that end, wavelet leader based characterization of texture is first recalled in Section 2. In the present work, multifractal properties are quantified using multiscale quantity $C_{1,j}$ that quantifies the evolution along analysis scales 2^j of the empirical mean of the log of the wavelet leaders at a given scale. This function is deeply related to the average or global regularity of the texture. Thus, it does not account for the entire multifractal properties of the texture, but provides us with a satisfactory partial description of multifractal properties that can be involved into texture segmentation. The multivariate segmentation procedure is detailed in Section 3. It consists of a multivariate Mumford-Shah relaxation formulated as a convex optimization problem involving a tensor structure penalization. An efficient algorithmic solution based on primal-dual proximal algorithm is proposed in Section 4. In Section 5, preliminary results are conducted on synthetic textures, designed to have piecewise constant multifractal properties.

2. MULTIFRACTAL ANALYSIS

Local regularity and multifractal spectrum. We denote $X = (X_\ell)_{1\leq \ell \leq N}$ the image to analyze having N pixels.

Work supported by GdR 720 ISIS under the junior research project GALILEO and ANR AMATIS grant #112432, 2010-2014

Its local regularity around position $\underline{\ell}$ can be quantified by the Hölder exponent $h_{\underline{\ell}}$: while large $h_{\underline{\ell}}$ points to a locally smooth portion of the field, low $h_{\underline{\ell}}$ indicates local high irregularity. Texture regularity fluctuations can be described by the so-called multifractal spectrum $\mathcal{D}(h)$ that describes the fluctuations of $h_{\underline{\ell}}$ along space in a global and geometrical manner (cf. e.g., [16, 5, 1] for details). For practical purposes, the multifractal spectrum can often be approximated as a parabola: $\mathcal{D}(h) = 2 + (h - c_1)^2/(2c_2)$. The practical estimation of $\mathcal{D}(h)$ requires the use of wavelet leaders.

Wavelet leaders. We denote $d^{(m)}_{j,\underline{k}} = \langle X, \psi^{(m)}_{j,\underline{k}} \rangle$ the (L^1-normalized) 2D discrete wavelet coefficients of X at location $\underline{k} = 2^{-j}\underline{\ell}$, at scale 2^j with $j \in \{1, \ldots, J\}$, and where m stands for the horizontal/vertical/diagonal subband. For a detailed definition of the 2D-DWT, readers are referred to e.g., [17].

Wavelet leaders were recently introduced [16, 5] to permit an accurate characterization of the multifractal properties of a texture. The wavelet leader $L_{j,\underline{k}}$, located around position $\underline{\ell} = 2^j\underline{k}$, is defined as the local supremum of all wavelet coefficients taken within a spatial neighborhood across all finer scales $2^{j'} \leq 2^j$, that is,

$$L_{j,\underline{k}} = \sup_{\substack{m=1,2,3,\\ \lambda_{j',\underline{k}'} \subset \Lambda_{j,\underline{k}}}} |d^{(m)}_{j',\underline{k}'}|, \tag{1}$$

with $\lambda_{j,\underline{k}} = [\underline{k}2^j, (\underline{k}+1)2^j)$ and $\Lambda_{j,\underline{k}} = \bigcup_{p\in\{-1,0,1\}^2} \lambda_{j,\underline{k}+p}$ [16, 5].

Multifractal analysis. We define $C_{1,j} \in \mathbb{R}^N$ and $C_{2,j} \in \mathbb{R}^N$ as the sample estimates of the mean and variance of the variable $\ln L_j$, i.e., averages across space $\underline{\ell}$ at each given scale 2^j. It has been shown that functions $C_{1,j}$ and $C_{2,j}$ are related to the multifractal spectrum $\mathcal{D}(h)$ via the coefficients c_1 and c_2 involved in its approximate expansion [1]:

$$\mathbb{E}C_{1,j} = c_1^0 + c_1 \ln 2^j, \tag{2}$$
$$\mathbb{E}C_{2,j} = c_2^0 + c_2 \ln 2^j. \tag{3}$$

Multifractal segmentation. To segment textures, one could naturally consider estimating $C_{1,j}$ and $C_{2,j}$ locally in a neighborhood of each pixel $\underline{\ell}$, estimate the corresponding local parameters $c_{1,\underline{\ell}}$ and $c_{2,\underline{\ell}}$, and then perform a multivariate segmentation of $\{c_{1,\underline{\ell}}, c_{2,\underline{\ell}}\}$. This, however, relies on the strong assumption that real-world textures follow precisely the scaling behaviors prescribed in Eqs. (2) and (3) above. In the present contribution, it has been chosen to relax this requirement. Therefore, the proposed segmentation relies on the multiscale function $C_{1,j} = \big(C_{1,j,\underline{\ell}}\big)_{1\leq\underline{\ell}\leq N}$ as a function of scales 2^j, defined as a local sample mean estimate,

$$C_{1,j,\underline{\ell}} = \frac{1}{|S_{j,\underline{\ell}}|} \sum_{\underline{k}' \in S_{j,\underline{\ell}}} \ln L_{j,\underline{k}'}, \tag{4}$$

where $S_{j,\underline{\ell}}$ denotes a (small) spatial neighborhood of $\underline{\ell} = 2^j\underline{k}$ at scale 2^j and where $|S_{j,\underline{\ell}}|$ is the number of coefficients in that neighborhood.

3. MULTIVARIATE SEGMENTATION

Original formulation. The original Mumford-Shah problem consists in labeling an image Y into Q distinct areas having a mean value of v_q, with by convention $v_q \leq v_{q+1}$. The minimization problem is

$$\min_{\Omega_1,\ldots,\Omega_Q} \sum_{q=1}^{Q} \int_{\Omega_q} (Y - v_q)^2 dx + \frac{1}{2}\sum_{q=1}^{Q} \mathrm{Per}(\Omega_q)$$
$$\text{subj. to} \quad \begin{cases} \bigcup_{q=1}^{Q} \Omega_q = \Omega, \\ (\forall q \neq p),\ \Omega_q \cap \Omega_p = \emptyset, \end{cases} \tag{5}$$

where the penalization $\mathrm{Per}(\Omega_q)$ imposes the solution to have a minimal perimeter and the constraints over the Q areas ensure non-overlapping of the partition.

In several work [18, 19], a relevant convexification of this criterion has been proposed. The resulting minimization problem is specified for our study where the usual univariate quantity Y is replaced by the multivariate $(C_{1,j})_{1\leq j\leq J}$, so that Eq. (5) consists in labeling $C_{1,j}$ by estimating, for every $q \in \{1, \ldots, Q+1\}$, $\Theta_q = (\theta_{q,j})_{1\leq j\leq J} \in \mathbb{R}^{JN}$ such that

$$\underset{\Theta_1,\ldots,\Theta_{Q+1}}{\text{minimize}} \sum_{q=1}^{Q}\sum_{j=1}^{J} (\theta_{q,j} - \theta_{q+1,j})^\top (C_{1,j} - v_{q,j})^2$$
$$+ \lambda \sum_{j=1}^{J}\sum_{q=1}^{Q} \mathrm{TV}(\theta_{q,j})$$
$$\text{subj. to} \quad \begin{cases} \Theta_1 = 1, \\ \Theta_{Q+1} = 0, \\ 1 \geq \Theta_2 \geq \ldots \geq \Theta_Q \geq 0, \end{cases} \tag{6}$$

where $\lambda > 0$ and where TV denotes the usual total-variation penalization as defined in [20], i.e., for every $\theta \in \mathbb{R}^N$,

$$\mathrm{TV}(\theta) = \sum_{\underline{\ell}=1}^{N} \|(D\theta)_{\underline{\ell}}\|_2 \tag{7}$$

where $D \in \mathbb{R}^{2N\times N}$ denotes the discrete horizontal/vertical difference operator and thus $(D\theta)_{\underline{\ell}} \in \mathbb{R}^2$. The choice of $v_{q,j} \in \mathbb{R}$ will be discussed later. It clearly appears that this criterion, separable over j, does not impose coupling between the scales 2^j.

Proposed solution. We propose to introduce correlations by modifying the criterion as

$$\underset{\Theta_1,\ldots,\Theta_{Q+1}}{\text{minimize}} \sum_{q=1}^{Q}\sum_{j=1}^{J} (\theta_{q,j} - \theta_{q+1,j})^\top (C_{1,j} - v_{q,j})^2$$
$$+ \lambda \sum_{q=1}^{Q} \mathrm{STV}(\Theta_q)$$
$$\text{subj. to} \quad \begin{cases} \Theta_1 = 1, \\ \Theta_{Q+1} = 0, \\ 1 \geq \Theta_2 \geq \ldots \geq \Theta_Q \geq 0, \end{cases} \tag{8}$$

where, for every $q \in \{1, \dots, Q\}$, the structure tensor penalization reads

$$\mathrm{STV}(\Theta_q) = \sum_{\underline{\ell}=1}^{N} \|\zeta_{q,\underline{\ell}}\|_p \quad \text{with} \quad p \geq 1$$

and where $\zeta_{q,\underline{\ell}} = (\zeta_{q,\underline{\ell},1}, \zeta_{q,\underline{\ell},2}) \in \mathbb{R}^2$ is defined from the singular value decomposition of $(D\theta_{q,\cdot})_{\underline{\ell}} \in \mathbb{R}^{J\times 2}$ that is

$$(D\theta_{q,\cdot})_{\underline{\ell}} = U_{q,\underline{\ell}} X_{q,\underline{\ell}} (V_{q,\underline{\ell}})^\top \tag{9}$$

where

$$\begin{cases} (U_{q,\underline{\ell}})^\top U_{q,\underline{\ell}} = \mathrm{Id}_J, \\ V_{q,\underline{\ell}} (V_{q,\underline{\ell}})^\top = \mathrm{Id}_2, \\ X_{q,\underline{\ell}} = \begin{pmatrix} \zeta_{q,\underline{\ell},1} & 0 & \dots & \dots & 0 \\ 0 & \zeta_{q,\underline{\ell},2} & 0 & \dots & 0 \end{pmatrix}^\top. \end{cases} \tag{10}$$

This multivariate formulation could be interpreted as a discrete version of the relaxation proposed in [12].

4. PRIMAL-DUAL ALGORITHM

Reformulation To propose an efficient algorithm for minimizing such a criterion, we first rewrite (8) as

$$\underset{\Theta=(\Theta_2,\dots,\Theta_Q)}{\text{minimize}} \sum_{q=2}^{Q}\sum_{j=1}^{J} \theta_{q,j}^\top \Big((C_{1,j} - v_{q,j})^2 - (C_{1,j} - v_{q-1,j})^2 \Big)$$
$$+ \lambda \sum_{q=2}^{Q} \mathrm{STV}(\Theta_q) + \iota_{E_0}(\Theta) + \iota_{E_1}(\Theta) + \iota_{E_2}(\Theta) \tag{11}$$

where, for every $k \in \{0,1,2\}$, ι_{E_k} denoted the indicator function of the non-empty closed convex set $E_k \subset \mathbb{R}^{(Q-1)JN}$, that is $\iota_{E_k}(\Theta) = 0$ if $\Theta \in E_k$ and $+\infty$ otherwise. E_0 denotes a dynamic range constraint that imposes Θ to belong to $[0,1]^{(Q-1)JN}$, i.e.,

$$E_0 = \{\Theta \in [0,1]^{(Q-1)JN}\}$$

and where

$$E_1 = \Big\{ \Theta \in \mathbb{R}^{(Q-1)JN} \,|\, \Theta_{2q} - \Theta_{2q+1} \geq 0, \quad (\forall q \in \{1, \dots, \lfloor (Q-1)/2 \rfloor\}) \Big\} \tag{12}$$

and

$$E_2 = \Big\{ \Theta \in \mathbb{R}^{(Q-1)JN} \,|\, \Theta_{2q+1} - \Theta_{2q+2} \geq 0, \quad (\forall k \in \{1, \dots, \lfloor (Q-2)/2 \rfloor\}) \Big\}. \tag{13}$$

Criterion (11) is the sum of five convex, lower-semicontinuous and proper functions, possibly non-smooth, and whose structure tensor penalization involves a linear operator. We thus propose iterations resulting from the proximal algorithm introduced in [21, 22]. The iterations are summarized in Algorithm 1. Under some technical assumptions insuring the existence of a solution (see [21, 22]), the iterates $\big(\Theta^{[n]}\big)_{n\in\mathbb{N}}$ converges to the minimizer of (11).

Algorithm 1 Multivariate segmentation algorithm.

Initialization
- Set $\tau > 0$ and $\sigma \in \Big]0, \tau^{-1}\big(\|D^\top D\| + 3\big)^{-1}\Big[$.
- Set $\Theta^{[0]} = (\theta_{q,j}^{[0]})_{2\leq q\leq Q, 1\leq j\leq J} \in \mathbb{R}^{(Q-1)JN}$
- Set $\widetilde{y}^{[0]} \in \mathbb{R}^{(Q-1)J(2N)}$ and $\widetilde{\widetilde{y}}^{[0]}, \bar{y}^{[0]}, \bar{\bar{y}}^{[0]} \in \mathbb{R}^{(Q-1)JN}$

For $n = 0, 1, \dots$
- *Primal steps: update $\theta^{[n+1]}$*
- For each $q \in \{2, \dots, Q\}$
  - For each $j \in \{1, \dots, J\}$
    - $z_{q,j}^{[n]} = \theta_{q,j}^{[n]} - \tau\big(D^\top \widetilde{y}_{q,j}^{[n]} - \widetilde{\widetilde{y}}_{q,j}^{[n]} - \bar{y}_{q,j}^{[n]} - \bar{\bar{y}}_{q,j}^{[n]}\big)$
- $\Theta^{[n+1]} = P_{E_0} z^{[n]}$
- $\widetilde{\Theta}^{[n+1]} = 2\Theta^{[n+1]} - \Theta^{[n]}$
- *Dual steps: update $\widetilde{y}^{[n+1]}$, $\widetilde{\widetilde{y}}^{[n+1]}$, $\bar{y}^{[n+1]}$, $\bar{\bar{y}}^{[n+1]}$*
- For each $q \in \{2, \dots, Q\}$
  - For each $j \in \{1, \dots, J\}$
    - $\widetilde{u}_{q,j}^{[n+1]} = \widetilde{y}_{q,j}^{[n]} + \sigma D\widetilde{\theta}_{q,j}^{[n+1]}$
- $\widetilde{\widetilde{u}}^{[n+1]} = \widetilde{\widetilde{y}}^{[n]} + \sigma\widetilde{\Theta}^{[n+1]}$
- $\bar{u}^{[n+1]} = \bar{y}^{[n]} + \sigma\widetilde{\Theta}^{[n+1]}$
- $\bar{\bar{u}}^{[n+1]} = \bar{\bar{y}}^{[n]} + \sigma\widetilde{\Theta}^{[n+1]}$
- For each $q \in \{2, \dots, Q\}$
  - For each $\underline{\ell} \in \{1, \dots, N\}$
    - Compute $\zeta_{q,\underline{\ell},1}^{[n+1]}$ and $\zeta_{q,\underline{\ell},2}^{[n+1]}$ from $\widetilde{u}_{q,\cdot,\underline{\ell}}^{[n+1]}$ (cf. (9))
    - $\eta_{q,\underline{\ell},\cdot}^{[n+1]} = \zeta_{q,\underline{\ell},\cdot}^{[n+1]} - \frac{\sigma}{\lambda}\mathrm{prox}_{\frac{\lambda}{\sigma}\|\cdot\|_p}(\frac{\lambda}{\sigma}\zeta_{q,\underline{\ell},\cdot}^{[n+1]})$
    - Compute $\widetilde{y}_{q,\underline{\ell}}^{[n+1]}$ from $\eta_{q,\underline{\ell},\cdot}^{[n+1]}$ (cf. (9))
  - For each $j \in \{1, \dots, J\}$
    - $\widetilde{\widetilde{y}}_{q,j}^{[n+1]} = \widetilde{\widetilde{u}}_{q,j}^{[n+1]} - \sigma\mathrm{prox}_{\sigma^{-1}\psi_{q,j}}(\sigma^{-1}\widetilde{\widetilde{u}}_{q,j}^{[n+1]})$
- $\bar{y}^{[n+1]} = \bar{u}^{[n+1]} - \sigma P_{E_1}(\sigma^{-1}\bar{u}^{[n+1]})$
- $\bar{\bar{y}}^{[n+1]} = \bar{\bar{u}}^{[n+1]} - \sigma P_{E_2}(\sigma^{-1}\bar{\bar{u}}^{[n+1]})$

Proximity operator. In Algorithm 1, the notation prox denotes the proximity operator [23]. For any convex, lower semi-continuous convex function φ from $\mathbb{R}^M$ to $]-\infty, +\infty]$, the proximity operator prox_φ is defined and reads, for every $u \in \mathbb{R}^M$, $\mathrm{prox}_\varphi(u) = \arg\min_{v\in\mathbb{R}^M} \frac{1}{2}\|u-v\|^2 + \varphi(v)$. When $\varphi = \iota_C$ with C being a non-empty closed convex subset of $\mathbb{R}^M$ then the proximity operator reduces to the projection, denoted P_C, onto the convex set.

The proximity operators involved in Algorithm 1 have a closed-form expression. Indeed, the closed form expression for $\mathrm{prox}_{\|\cdot\|_p}$ with $p = 2$ is given in [24], while the case $p = 1$ reduces to the soft-thresholding operator. Note that when $p = 2$, the singular value decomposition step could be avoided [25]. On the other hand, we have denoted

$$(\forall \theta \in \mathbb{R}^N) \quad \psi_{q,j}(\theta) = \theta^\top \Big((C_{1,j} - v_{q,j})^2 - (C_{1,j} - v_{q-1,j})^2 \Big)$$

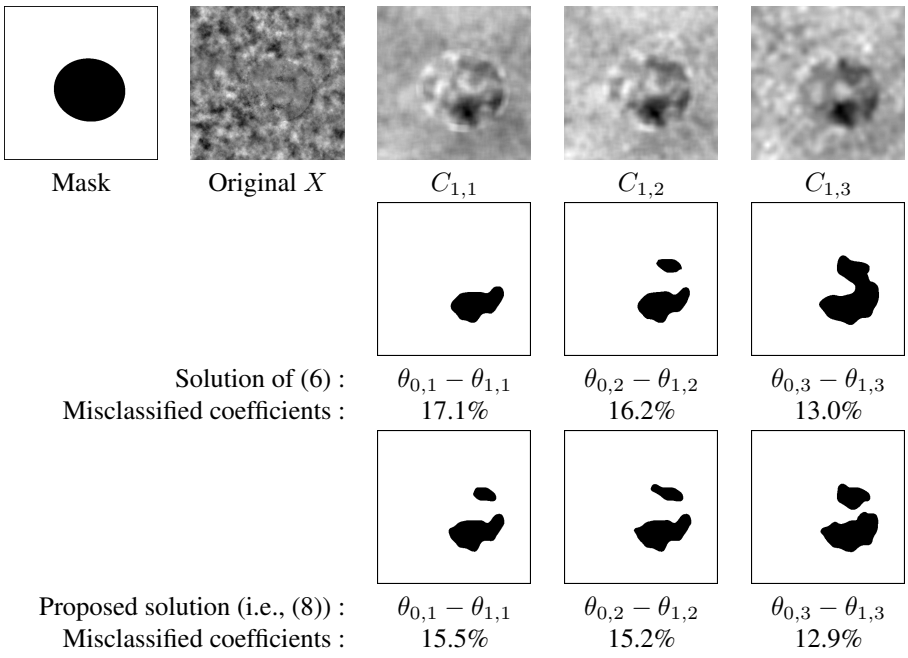

Fig. 1. Results of the proposed multivariate segmentation against a segmentation procedure done for each component separately. 1st line (left to right): mask allowing to generate the data, original data, estimates of the mean of $C_{1,j}$ for $j = 1$, $j = 2$, and $j = 3$. 2nd line (left to right): Results of the segmentation procedure described in (6) for $j = 1$, $j = 2$, and $j = 3$. 3rd line (left to right): Results of the proposed segmentation procedure described in (8) for $j = 1$, $j = 2$, and $j = 3$.

whose proximity operator reduces to

$$\mathrm{prox}_{\sigma^{-1}\psi_{q,j}}\theta = \theta - \sigma^{-1}\Big((C_{1,j} - v_{q,j})^2 - (C_{1,j} - v_{q-1,j})^2\Big).$$

Finally, the projections onto E_0, E_1, and E_2 reduce to projection onto hyperslabs [26, Example 28.17]

Some other primal-dual solution could have been proposed such as the one derived in [27, 28]. For a summary on primal-dual strategies, the reader could refer to [29].

5. EXPERIMENTS

Performance of the proposed segmentation procedure are assessed on synthetic data, numerically produced by inclusion of a 2D-MRW patch [30] into a 2D-MRW background with different multifractal parameters: $(c_1, c_2) = (0.8, -0.005)$ and $(0.5, -0.05)$ respectively. Patch and background have been normalized to ensure that the local variance does not depend on the image location. An example of such texture is shown in Figure 1.

Our simulations are performed using a standard 2D DWT with orthonomal tensor product Daubechies mother wavelets with 2 vanishing moments over $J = 3$ scales. We propose to compare the performance of the proposed multivariate solution against a segmentation proceeded for each $C_{1,j}$ separately. In our simulations $Q = 2$, $\lambda = 20$, and $p = 2$. For every scale $j \in \{1, \ldots, J\}$, $(v_{q,j})_{1 \leq q \leq Q}$ are chosen to be equally distributed between the minimum and maximum values of $C_{1,j}$. The proposed solution, whose result is depicted in Fig. 1-(bottom line), achieves a smaller rate of misclassified coefficients for each scale, which illustrate the interest of such a multivariate approach. The information of each scale can then be combined to achieve a segmentation of the original texture X. Segmentation have been performed over several realizations and similar conclusions can be drawn.

6. CONCLUSIONS AND PERSPECTIVES

Elaborating on our previous works aiming to segment textures into local regularity piecewise constant regions, the contribution of the present work is twofold : (i) it constitutes a first attempt to achieve texture segmentation into regions, each characterized with homogeneous multifractal properties and (ii) it proposes a multivariate segmentation procedure to take into account correlations between several components.

Instead of making direct use of multifractal attributes parametrizing the multifractal spectrum (c_1, c_2,...), it has been chosen here to recourse to the multiscale quantity $C_{1,j}$ from which c_1 can theoretically be extracted.

We have shown that the multivariate (multiple scales) segmentation of $C_{1,j}$ permits to detect the change of texture through the scales in order to identify regions with homogeneous multifractal properties. These results on synthetic data thus pave the way to promising results on mixtures of fractal-like real-world textures (cloud and snow) previously investigated in [15]

7. REFERENCES

[1] H. Wendt, S.G. Roux, P. Abry, and S. Jaffard, "Wavelet leaders and bootstrap for multifractal analysis of images," *Signal Proces.*, vol. 89, pp. 1100–1114, 2009.

[2] C.L. Benhamou, S. Poupon, E. Lespessailles, S. Loiseau, R. Jennane, V. Siroux, W. J. Ohley, and L. Pothuaud, "Fractal analysis of radiographic trabecular bone texture and bone mineral density: two complementary parameters related to osteoporotic fractures," *J. Bone Miner. Res.*, vol. 16, no. 4, pp. 697–704, 2001.

[3] P. Abry, S. Jaffard, and H. Wendt, "When Van Gogh meets Mandelbrot: Multifractal classification of painting's texture," *Signal Process.*, vol. 93, no. 3, pp. 554–572, 2013.

[4] C. R. Johnson, P. Messier, W. A. Sethares, A. G. Klein, C. Brown, P. Klausmeyer, P. Abry, S. Jaffard, H. Wendt, S. G. Roux, N. Pustelnik, N. van Noord, L. van der Maaten, E. Postma, J. Coddington, L. A. Daffner, H. Murata, H. Wilhelm, S. Wod, and M. Messier, "Pursuing automated classification of historic photographic papers from raking light photomicrographs.," *Journal of the American Institute for Conservation*, vol. 53, no. 3, pp. 159–170, 2014.

[5] H. Wendt, P. Abry, and S. Jaffard, "Bootstrap for empirical multifractal analysis," *IEEE Signal Process. Mag.*, vol. 24, no. 4, pp. 38–48, Jul. 2007.

[6] M. Kass, A. Witkin, and D. Terzopoulos, "Snakes: Active contour models," *Int. J. Comp. Vis.*, vol. 1, no. 4, pp. 321–331, Jan. 1988.

[7] D. Mumford and J. Shah, "Optimal approximations by piecewise smooth functions and associated variational problems," *Comm. Pure Applied Math.*, vol. 42, pp. 577–685, 1989.

[8] V. Caselles, R. Kimmel, and G. Sapiro, "Geodesic active contours," in *Proc. IEEE Int. Conf. Comput. Vis.*, Boston, USA, 1995, pp. 694–699.

[9] S Kichenassamy, A. Kumar, P. J. Olver, A. Tannenbaum, and A. J. Yezzi, "Gradient flows and geometric active contour models," in *Proc. IEEE Int. Conf. Comput. Vis.*, 1995, pp. 810–815.

[10] T. F. Chan and L. A. Vese, "Active contours without edges," *IEEE Trans. Image Process.*, vol. 10, no. 2, pp. 266–277, 2001.

[11] C. Couprie, L. Grady, L. Najman, and H. Talbot, "Power watershed: A unifying graph-based optimization framework," *IEEE Trans. Pattern Anal. Match. Int.*, vol. 33, no. 7, pp. 1384–1399, Jul. 2011.

[12] E. Strekalovskiy, A. Chambolle, and D. Cremers, "A convex representation for the vectorial Mumford-Shah functional," in *IEEE Conference on Computer Vision and Pattern Recognition*, Providence, Rhode Island, June 2012.

[13] N. Pustelnik, P. Abry, and H Wendt, "Local regularity for texture segmentation : combining wavelet leaders and proximal minimization," in *Proc. Int. Conf. Acoust., Speech Signal Process.*, Vancouver, Canada, May 26-31 2013.

[14] N. Pustelnik, P. Abry, H Wendt, and N. Dobigeon, "Inverse problem formulation for regularity estimation in images," in *Proc. Int. Conf. Image Process.*, Paris, France, Oct. 27-30 2014.

[15] N. Pustelnik, H. Wendt, P. Abry, and N. Dobigeon, "Local regularity, wavelet leaders and total variation based procedures for texture segmentation," Apr. 2015, preprint, http://arxiv.org/abs/1504.05776.

[16] S. Jaffard, "Wavelet techniques in multifractal analysis," in *Fractal Geometry and Applications: A Jubilee of Benoît Mandelbrot, M. Lapidus and M. van Frankenhuijsen Eds., Proceedings of Symposia in Pure Mathematics*, M. Lapidus and M. van Frankenhuijsen, Eds. 2004, vol. 72, pp. 91–152, AMS.

[17] S. Mallat, *A wavelet tour of signal processing*, Academic Press, San Diego, USA, 1997.

[18] T. Chan, S. Esedoglu, and M. Nikolova, "Algorithms for finding global minimizers of image segmentation and denoising models," *SIAM Journal of Applied Mathematics*, vol. 66, no. 5, pp. 1632–1648, 2006.

[19] T. Pock, A. Chambolle, D. Cremers, and B. Horst, "A convex relaxation approach for computing minimal partitions," in *IEEE Conference on Computer Vision and Pattern Recognition*, Miami Beach, Florida, USA, Jun., 20-25 2009.

[20] A. Chambolle, "An algorithm for total variation minimization and applications," *J. Math. Imag. Vis.*, vol. 20, no. 1-2, pp. 89–97, Jan. 2004.

[21] B. C. Vũ, "A splitting algorithm for dual monotone inclusions involving cocoercive operators," *Adv. Comput. Math.*, vol. 38, pp. 667–681, 2011.

[22] L. Condat, "A primal-dual splitting method for convex optimization involving Lipschitzian, proximable and linear composite terms," *J. Optim. Theory Appl.*, vol. 158, no. 2, pp. 460–479, 2013.

[23] J. J. Moreau, "Proximité et dualité dans un espace hilbertien," *Bull. Soc. Math. France*, vol. 93, pp. 273–299, 1965.

[24] G. Peyré and J. Fadili, "Group sparsity with overlapping partition functions," in *Proc. Eur. Sig. Proc. Conference*, Barcelona, Spain, Aug. 29 – Sept. 2, 2011, pp. x+5.

[25] G. Chierchia, N. Pustelnik, B. Pesquet-Popescu, and J.-C. Pesquet, "A non-local structure tensor based approach for multicomponent image recovery problems," *IEEE Trans. Image Process.*, vol. 23, no. 12, pp. 5233–5248, Oct. 2014.

[26] H. H. Bauschke and P. L. Combettes, *Convex Analysis and Monotone Operator Theory in Hilbert Spaces*, Springer, New York, 2011.

[27] A. Chambolle and T. Pock, "A first-order primal-dual algorithm for convex problems with applications to imaging," *J. Math. Imag. Vis.*, vol. 40, no. 1, pp. 120–145, 2011.

[28] P. L. Combettes and J.-C. Pesquet, "Primal-dual splitting algorithm for solving inclusions with mixtures of composite, Lipschitzian, and parallel-sum type monotone operators," *Set-Valued Var. Anal.*, 2011.

[29] N. Komodakis and J.-C. Pesquet, "Playing with duality: An overview of recent primal-dual approaches for solving large-scale optimization problems," *IEEE Signal Processing Magazine*, 2014, accepted for publication.

[30] Raoul Robert, Vincent Vargas, et al., "Gaussian multiplicative chaos revisited," *The Annals of Probability*, vol. 38, no. 2, pp. 605–631, 2010.